Development of UNS S 32760 super-duplex stainless steel produced in large diameter rolled bars

Desenvolvimento do aço inoxidável super-duplex UNS S 32760 produzido em barras laminadas de grande diâmetro

Celso Antonio Barbosa
Engenheiro Metalurgista , Membro da ABM,
Diretor de Tecnologia e P&D ,
Villares Metals S. A., Sumaré - SP, Brasil.
celso.barbosa@villaresmetals.com.br.

Alexandre Sokolowski
Engenheiro químico, Mestre em Metalurgia,
Pesquisador Sênior,
Villares Metals S.A. Sumaré, SP, Brasil.
alexandre.sokolowski@villaresmetals.com.br.

Abstract

Nowadays super-duplex stainless is an important material for the Oil and Gas industries, especially for off-shore production. In deep water exploitation the reliability of production system is very important. Corrosion resistance for pitting of the high alloyed duplex stainless steels with high Mo and N content has to be achieved even in large diameters bars. Therefore, the present work deals with an improved super-duplex stainless steel for the production of large diameter rolled 6bars up to 152.40 mm (6 inches). Among the main improvements, the corrosion resistance evaluated both by the chemical method according to the ASTM G-48 method, as well as electrochemical methods, was achieved. During the production of such large dimensions, the precipitation of inter-metallics and nitrides after cooling from high temperatures was studied by changing the chemical composition using Thermo-Calc and evaluating the new proposed chemical compositions. Several alloy compositions were laboratory scale cast, and the austenite/ferrite balance as well as PREN pitting resistance equivalent number content was correlated to the microstructure and the corrosion properties obtained. It was thus possible to determine the ideal chemical composition and define the new processing parameters to produce the UNS S32760 grade (4501) according to the Norsok standard. The new material properties produced in a production full scale heat are also presented.

Keywords: Corrosion, super-duplex stainless steel, pitting.

Resumo

Os aços inoxidáveis superduplex, atualmente, são materiais importantes para a indústria de óleo e gás, especialmente para produção off-shore. Em águas profundas, a confiabilidade do sistema de produção é muito importante. A resistência à corrosão dos aços inoxidáveis duplex de alta liga com alto teor de Mo e N, especialmente em relação à corrosão por pite, tem de ser alcançada, até mesmo em barras com grandes diâmetros. Portanto o presente trabalho trata de um aço inoxidável superduplex com propriedades melhoradas para a produção de barras laminadas de grande diâmetro, ou seja, de até 152,40 milímetros (seis polegadas). Entre as principais melhorias, a resistência à corrosão, avaliada, tanto pelo método químico, de acordo com ASTM G-48, bem como pelos métodos eletroquímicos, foi alcançada. Durante a produção

de tais grandes dimensões, a precipitação de intermetálicos e nitretos, após o resfriamento das altas temperaturas, foi estudada através da alteração da composição química, usando o software Thermo-Calc e avaliando as novas composições químicas propostas. Várias composições de ligas foram fundidas, em escala de laboratório, e o equilíbrio austenita / ferrita, bem como o PREN, número equivalente de resistência ao pite, foram correlacionados com a microestrutura e as propriedades de corrosão obtidas. Foi possível determinar a composição química ideal e definir os novos parâmetros de processamento para produzir o UNS S 32760 grau (4501), de acordo com a norma NORSOK. As propriedades dos novos materiais produzidos, em uma escala de produção industrial, também são apresentadas.

Palavras-chave: *Corrosão, aço inoxidável superduplex, corrosão por pites.*

1. Introduction

The excellent combination of mechanical strength and corrosion resistance in various types of environments and the good performance in applications found in Oil and Gas fields makes duplex stainless steels (DSS) an excellent choice by equipment designers IMOA (2009). The development of more corrosion resistant grades has led to the so called Super-duplex stainless steels (SDSS), where the chemical composition is modified by increasing specially the molybdenum and nitrogen content, leading to a higher pitting corrosion resistance, evaluated by the pitting resistance equivalent number – PREN, from a typical value of 35, found in normal duplex grades, to more than 40. This new class of DSS can fight the more challenging corrosion problems found in the nowadays deep water oil and gas reserves where, besides temperature increases, higher H_2S and CO_2 pressures are met (Løvland, 2003). Also, besides the supermartensitic 13Cr, the SDSS shows the best combination of corrosion resistance and yield strength ultrapasses 600 MPa (Barbosa, 2008). From the metallurgical point of view and also processing characteristics, the SDSS production in large diameters bars is a challenge because their attractive properties may be destroyed by the formation of precipitates due to the more difficult thermal transfer conditions found in bars with diameters higher than 100 mm. The most common precipitates are chromium nitrides Cr_2N and intermetallic precipitates (IP) such as sigma/chi/phase/R phases that can be formed in the temperature range from 600 to 1000°C, depending on the thermal cooling as well as deformation conditions imposed during the fabrication of large diameter bars. The main technological properties that are adversely affected are the pitting corrosion resistance and the toughness. It is interesting to note that in the present study, although the pitting corrosion resistance was damaged by the presence of chromium nitrides, the minimum impact toughness was not affected when a very small percentage of IP is present in the microstructure, confirming previous work showing that to have a serious decrease in toughness several percent of IP is necessary (Nilsson & Kangas, 2007). Also important is the control of the ferrite/austenite balance (usually near 50% each) that can be established by a proper compositional balance between ferrite and austenite former elements. The knowledge of the thermodynamic and kinetics of such complex stainless steels is a pre-condition to understand and control the formation of such undesirable precipitates. Many of these aspects are very well studied and documented in literature (DUPLEX, 2007).

In order to investigate the reasons why corrosion resistance is sometimes affected in the production of SDSS in large diameter bars over 80 mm, we conducted an extensive study in the grade UNS S 32760 ASTM A-276 (4501), see Table 1. The main task was to fulfill the additional requirements found in the Norsok standard MDS D57 Revision 3, especially regarding pitting corrosion. The production bars were produced by rolling conventional cast ingots from EAF+VOD process. After controlled rolling, the bars were water solution annealed from 1120°C.

2. Experimental Procedure

Pilot scale heats were produced in order to verify the compositional effects on the microstructures and corrosion as well as to study the effect of the chemical composition balance. The pilot scale heats were produced by casting 50 kg ingots from a vacuum induction furnace, with 140 mm medium cross section size. All heats were cast using the same raw material and were forged together using the same heating condition. The chemical compositions were established using as a base the typical composition found in heats from regular production in order to run the thermodynamic phase simulation using the software Thermo-Calc. The ingots were further forged down to 70 mm square bars with a 4:1 reduction ratio. The chemical composition of the produced ingots is given also in Table 1. The conventional base composition was reproduced in the pilot scale heat and it is indicated as well as the modified ones. In the rebalanced composition the PREN number was increased via chromium and molybdenum to more than 41. The content of ferrite in the conventional steel, around 57%, was reduced to around 42% in the rebalanced composition in the solution annealing temperature of 1120°C as calculated by the Thermo-Calc. The higher amount of austenite promotes a higher ductility and toughness (Esteban, 2008).

The specimens were cut from the middle section of the 70 mm square bar and exposed to pilot heats to control the microstructure and corrosion testing. In the production heats the samples were taken at different positions of the 152.40 mm diameter rolled bars. The production heats were produced by EAF+VOD and 1.7 t ingot cast. The materials were water solution annealed from 1120°C. The specimens for corrosion testing according ASTM G-48 method A (AMERICAN SOCIETY FOR TESTING AND MATERIALS, 2007) and Norsok standard were taken from the mid radius in the

longitudinal direction and had the surface polished to # 120 grit. The temperature of testing was continuously monitored and recorded, as can be seen in Figure 1. Also the CPT-Critical Pitting Temperature was determined using the potentiodynamic method. The determination of the critical pitting temperature (CPT) was conducted according to ASTM G 150-99 (AMERICAN SOCIETY FOR TESTING AND MATERIALS, 2009) (using the same solution recommended in ASTM G-48-03, method E). All determinations were made in duplicate. The corrosion samples were submitted to optical microscopy and SEM. To identify the austenite and ferrite phases, NaOH electrolytic etchant (20g NaOH and 80 ml distilled H_2O) was applied. Light optical microscopy (LOM) was performed in a Zeiss inverted microscope in the transversal specimen direction. A 95% confidence interval of the volume fractions of ferrite, austenite and inter-metallic phase was estimated using manual point counting according to the standardized ISO 9042 procedure.

Steel	UNS S 32760	Conventional Heat H -7263	Pilot Scale Heats		Production Heat Rebalanced H-7441
			Conventional (Average) H-604	Rebalanced H-607	
C	Max 0.03	0.019	0.02	0.017	0.024
Si	Max 1.0	0.38	0.42	0.4	0.35
Mn	Max 1.0	0.7	0.69	0.6	0.6
Cr	24 - 26	24.9	24.8	25.3	25.3
Ni	6 - 8	6.38	6.54	6.85	6.84
Mo	3 - 4	3.37	3.37	3.68	3.55
N	0.2 - 0.3	0.27	0.28	0.26	0.25
P	Max 0.03	0.026	0.026	0.026	0.017
S	Max 0.01	0.001	0.001	0.003	< 0.001
Cu	0.5 – 1.0	0.63	0.64	0.6	0.54
W	0.5- 1.0	0.65	0.65	0.7	0.63
PREN	≥ 40.0	40.3	40.4	41.6	41.02

Table 1
Chemical composition of super-duplex stainless steel UNS 32760-ASTM A276 standard (4501)), the pilot scale heats and the rebalanced new production heat produced (% in mass).

Figure 1
Apparatus for determination of pitting resistance according ASTM G-48 method A, showing the temperature recorder of the control thermocouples.

3. Results and Discussion

The simulations using Thermo-Calc are shown in Figure 2 and 3 for the compositions of the conventional and the rebalanced steels. Two points should be observed: the higher amount of austenite in the rebalanced steel, see dotted lines in the figures corresponding to the usual solution annealing temperature of 1120°C for this grade, and the chromium nitride precipitation is depressed to lower temperatures (~1040°C) relative to the conventional steel(~1190°C). Hot processing of super-duplex steels like rolling and forging of large diameters bars should ideally led to conditions of finishing process temperatures over the chromium nitride temperature precipitation, as shown by simulation.

Table 2 presents the amount of ferrite predicted by Thermo-Calc and the amount found in the samples of the production conventional and rebalanced steels compositions, showing a good fit.

The conventional steel showed a high corrosion mass loss in the G-48 immersion test as can be seen in Table 3 for three different diameter bars and heats and with heavy presence of pitting on the specimen surface, Figure 4.

The optical microstructure and SEM of the corroded surfaces indicated that the pitting initiation occurred in the ferrite grain boundaries, Figures 5, 6 and 7. Figure 5 is the SEM examination of the G-48 corrosion specimen surface just after testing showing that the pitting initiation is concentrated in the ferrite grains.

At larger magnification, as showed in Figure 6, it was possible to observe

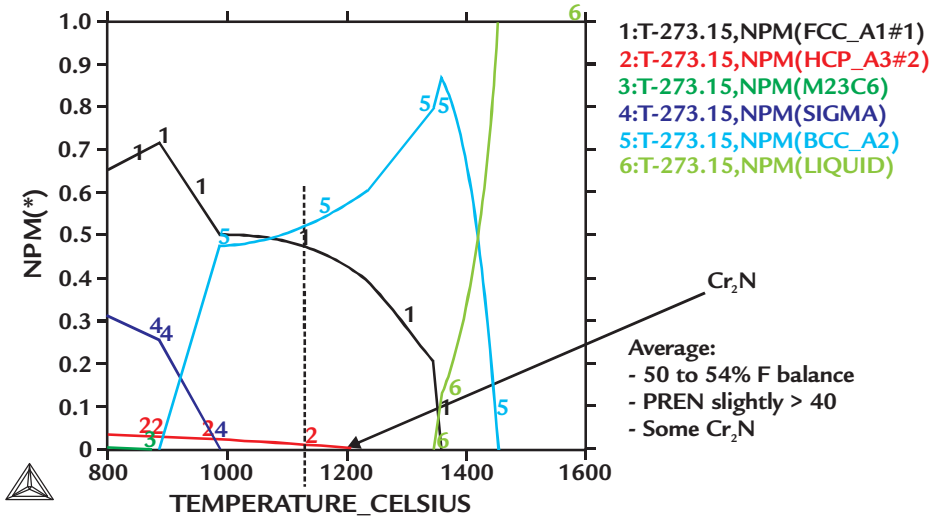

Figure 2
Equilibrium microstructure constituents predicted by the Thermo-Calc software for the conventional production steel average composition (molar %). Dotted line indicates the solution annealing temperature of 1120°C. Note a predominant ferrite microstructure is predicted.

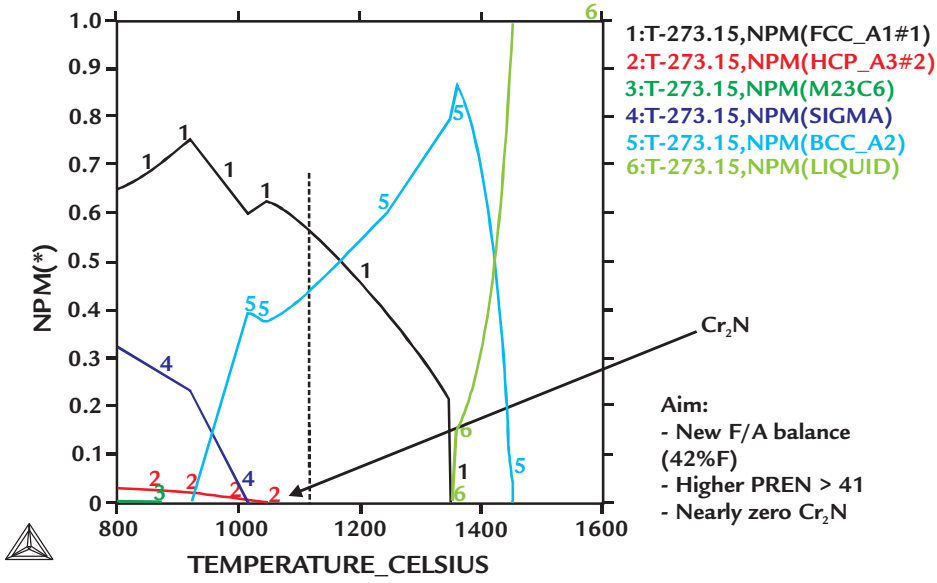

Figure 3
Equilibrium microstructure constituents predicted by the Thermo-Calc software for the rebalanced composition (molar %). Notice in line 2 the predicted temperature of Cr_2N is depressed to lower temperature. Dotted line indicates the solution annealing temperature of 1120°C.

Steel	Ferrite (%)	
	Predicted	Real
Conventional	52	57.5
Rebalanced	42	41.3

Table 2
Predicted and real volume fraction of ferrite for conventional and rebalanced steels, at 1120°C.

Sample	Mass Loss (g/m²)
612 (∅ 127.0 mm)	10.7 / 15.6
651 (∅ 95.25 mm)	50.9 / 64.8
606 (∅ 82.55 mm)	28.1 / 67.3

Table 3
Mass losses in three samples of the conventional steel after 24 h at 50°C showing values above the maximum allowed by Norsok standard of 4.0 g/m².

Figure 4
Conventional steel corrosion surface of the G 48 specimen 606 after 24 h at 50°C showing the pits.

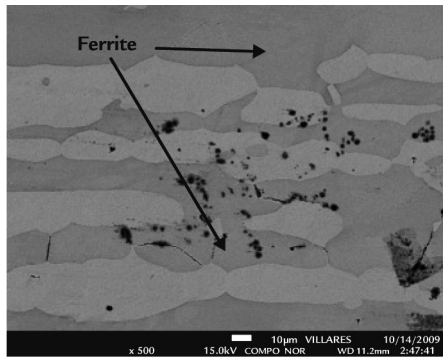

Figure 5
Compositional SEM image of the corrosion specimen surface without etching showing the pitting initiation is concentrated in the ferrite. Longitudinal direction. Magnification 500X.

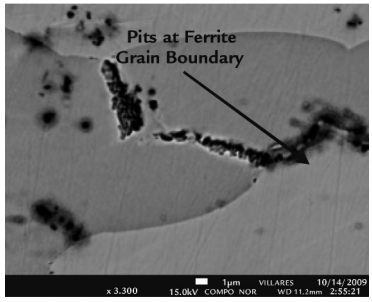

Figure 6
Compositional SEM image of the corrosion specimen surface without etching showing the pitting initiation in the ferrite grain boundaries. Longitudinal direction. Magnification 3,300 X.

that most of the ferrite grain boundaries had pitting initiation. In order to identify the presence of phases in the ferrite grain boundaries, the same corrosion sample was polished and etched to be observed in the SEM. Figure 7 shows the presence of grain boundary precipitates detected by the compositional image (indicated by darker points of lighter chemical elements comparative to the matrix). The EDS profiles of such precipitates indicate the presence of higher intensities values of Cr and N, indicative of chromium nitride precipitation, Figure 8.

The Figure 9(A) shows a typical microstructure of one of the production conventional heats showing the intensive ferrite grain boundary precipitation of Cr_2N and the predominance of ferrite phase with some secondary austenite.

The microstructure of the pilot scale heat with its composition adjusted to reproduce the average chemical composition of the conventional production heats is shown in Figure 9(B). The same intergranular precipitation can be seen inside the ferrite grains.

Figure 9(C) is the microstructure of the rebalanced composition pilot scale heat. It is clear the absence of precipitation inside the ferrite grains as observed in the LOM.

The corrosion behavior of the pilot scale heats were checked using also the G-48 immersion test. Table 4 shows the results obtained in the conventional heat H-604 with a reproduction of the conventional chemical composition and the results of the rebalanced steel, pilot scale heat H-607. The improvement in corrosion values of the rebalanced steel is quite well evident in relation to the conventional steel and is far below the maximum allowed by Norsok standard of 4.0 g/m^2.

The production rebalanced steel showed an impressive improvement in mass loss in the G-48 immersion test as can be seen in Table 5 for a 152.40 mm diameter bar tested in three different bar positions with no occurrence of pitting on the corrosion specimen surface, Figure 10.

The microstructure obtained in the production rebalanced steel is presented in Figure 11. It is evident the improvement when comparing the ferrite grains free of precipitation and higher amount of austenite.

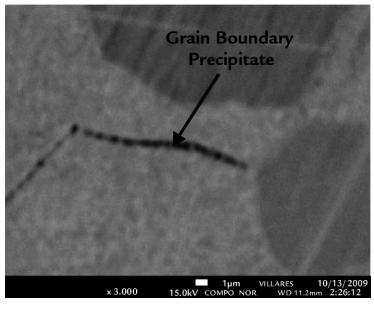

Figure 7
Compositional image of SEM image showing ferrite grain boundaries precipitates with size less than 1.0 micron in a polished sample of conventional steel. Longitudinal direction. Magnification 3,000 X.

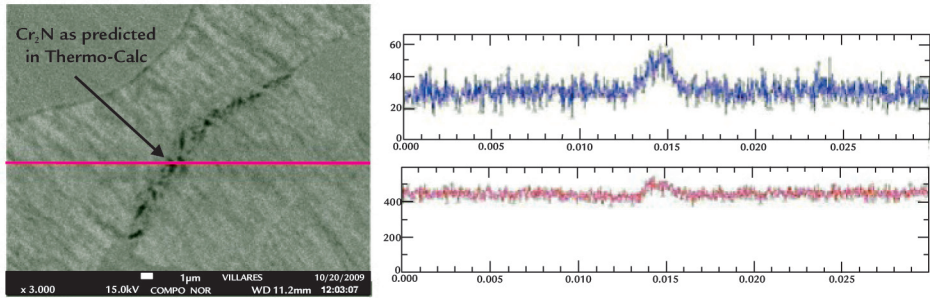

Figure 8
Ferrite grain boundary precipitation analyzed by EDS showing the presence of N and Cr in the precipitate. Longitudinal direction. Magnification 3,000 X.

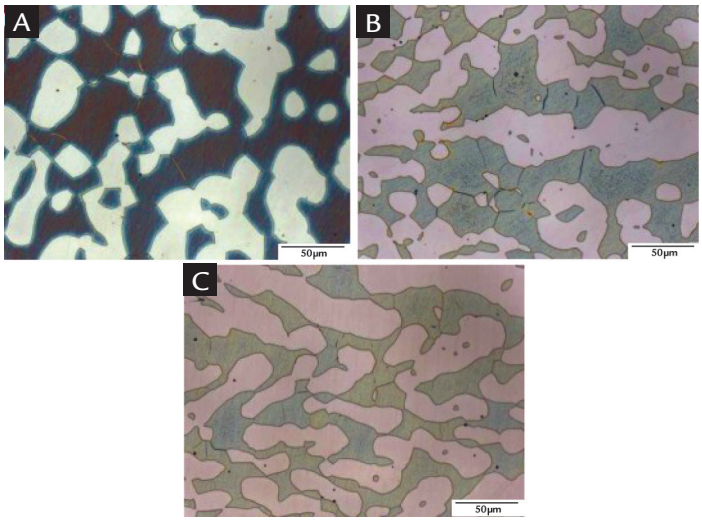

Figure 9
Microstructure of the bars. (A) 127.0 mm diameter bar of conventional production heat (H-7263/Sample 651) that failed in passing in the corrosion testing ASTM G-48 showing the presence of precipitates in the ferrite grain boundaries and the presence of some secondary austenite, (B) conventional steel pilot scale heat H-604 showing the presence of precipitates in the ferrite grain boundaries and the presence of secondary austenite, (C) rebalanced composition steel pilot scale heat H-607 showing only the presence of ferrite with grain boundaries without nitrides precipitates, austenite and small presence of secondary austenite. All microstructure in the transversal direction. Electrolytic NaOH etching. Magnification 500 X.

Pilot Heat	Mass Loss (g/m²)
604 - Conventional	6.35
607 - Rebalanced	0.13

Table 4
G-48 ass losses in the conventional and rebalanced steels pilot scale heats after 24 h at 50°C.

Sample Position	Mass Loss (g/m²)	
	Individual Values	Average
Center of Bar End	0.06	0.09 ± 0.03
Mid Radius of Bar Middle	0.09	
Center of Bar Middle	0.12	

Table 5
G-48 mass losses of 152.40 mm bar determined in three pozsitions of the rebalanced steel after 24 h at 50°C showing values far below the maximum allowed by Norsok standard of 4.0 g/m².

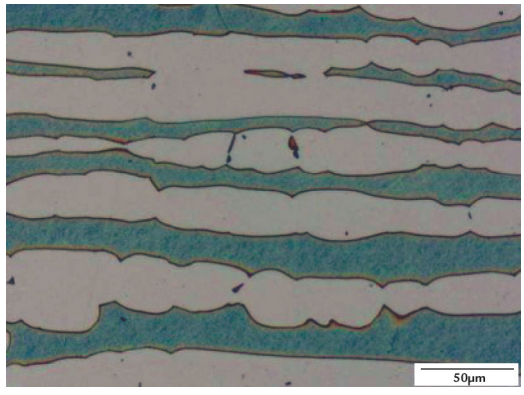

Figure 10
G-48 corrosion specimen of the rebalanced steel after 24 h at 50°C showing no pits on the testing surface.

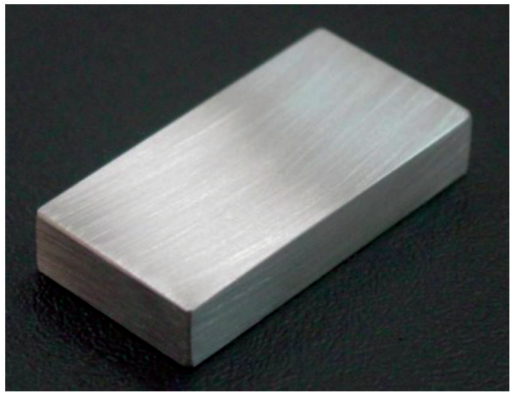

Figure 11
Microstructure of 152.40 mm diameter bar of rebalanced production heat (H-7441/Sample 430) that passed in the corrosion testing ASTM G-48 showing no presence of precipitates in the ferrite grain boundaries. Center of the bar middle. Longitudinal direction. Electrolytic NaOH etching. Magnification 500 X.

Table 6 shows the critical pitting temperature-CPT of the production conventional and rebalanced steel. It is observed that rebalanced steel shows a higher pitting corrosion resistance when compared to the conventional steel. A CPT increase of more than 20 °C was observed. The difference of CPT temperature could not be only explained by the slight increase in PREN values. Based on the metallographic evidences on pitting initiation at the ferrite grain boundaries with Cr_2N

precipitation in the conventional steel, we evaluated the amount of precipitates in both steels. Table 7 shows the Cr_2N percentages found. The rebalanced steel showed no evidence of Cr_2N precipitation in ferrite grain boundaries both in LOM as well as in SEM.

The relationship between Cr_2N precipitation in the ferrite grain boundaries and CPT can be seen in Figure 12. The reduction of CPT temperature near to 50°C explains why the G-48 test developed a high pitting level in the corrosion specimens, as showed in Figure 4 and an inacceptable mass loss, Table 3.

The PREN can be calculated using the Thermo-Calc simulation that gives us the chemical compositions of the equilibrium phases present in the steel at each temperature. The chemical composition of austenite and ferrite were calculated in three different temperatures including the recommended solution annealing temperature for this steel grade of 1120°C. Figure 13 shows the calculation results for the temperatures of 1050, 1120 and 1200°C. The first observation is that the austenite PREN is lower than ferrite PREN and tends to reach the ferrite number only at high temperatures, near 1200°C. Second, the rebalanced steel shows a PREN number both in austenite as in ferrite higher than the conventional steel.

As Thermo-Calc gives also the phase molar fraction, we have also estimated the PREN total of each steel composition, considering only the austenite and ferrite phases. The calculated total PREN value is higher than 40 at 1120°C for the rebalanced steel, Figure 14, showing that the compositional changes introduced led to a good combination of stronger corrosion resistant austenite and ferrite in a proper balance, increasing the corrosion resistance of the rebalanced steel.

In the Table 8 we can observe the improvement in toughness as evaluated by the absorbed impact energy. It is interesting to notice that the minimum required value was obtained even in the conventional steel that failed in corrosion, showing that the improper austenite/ferrite balance and chromium nitride precipitation did not deteriorate the toughness to a level under the specified values.

Table 6
Critical pitting temperatures values determined using potentiostatic method of the conventional and rebalanced steels.

Steel	CPT – Critical Pitting Temperature (°C)			
	Individual Values		Average	
Conventional	53	55	60	56
Rebalanced	73	85	-	76

Table 7
Amount of Cr_2N precipitated at ferrite grain boundaries in the conventional and rebalanced steels.

Steel	Cr_2N GBP (%)
Conventional	0.84 ± 0.14
Rebalanced	0.01

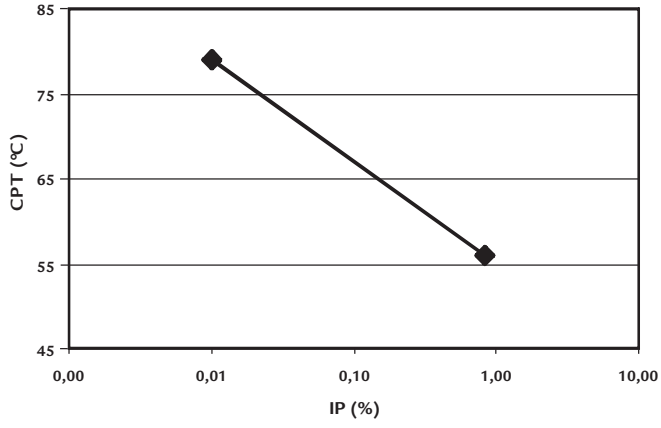

Figure 12
Effect of the amount of Cr_2N intergranular precipitation on the Critical Pitting Temperature-CPT determined by potentiostatic method (average values).

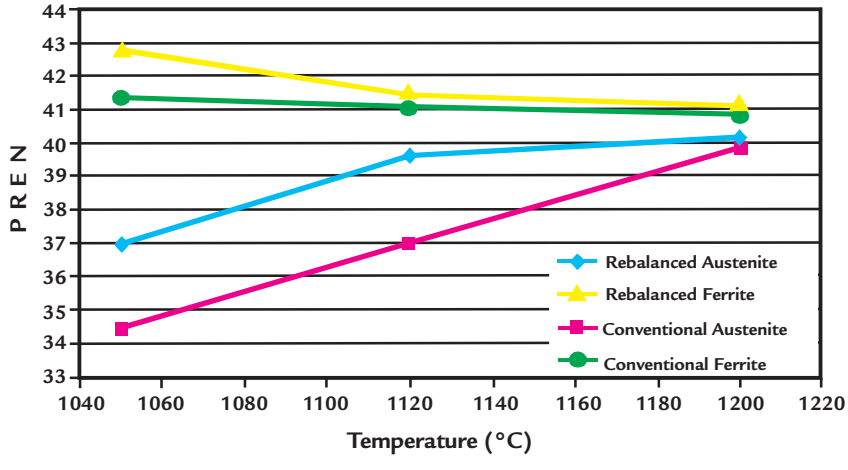

Figure 13
Ferrite and Austenite PREN number for the Conventional and Rebalanced steel calculated by Thermo-Calc.

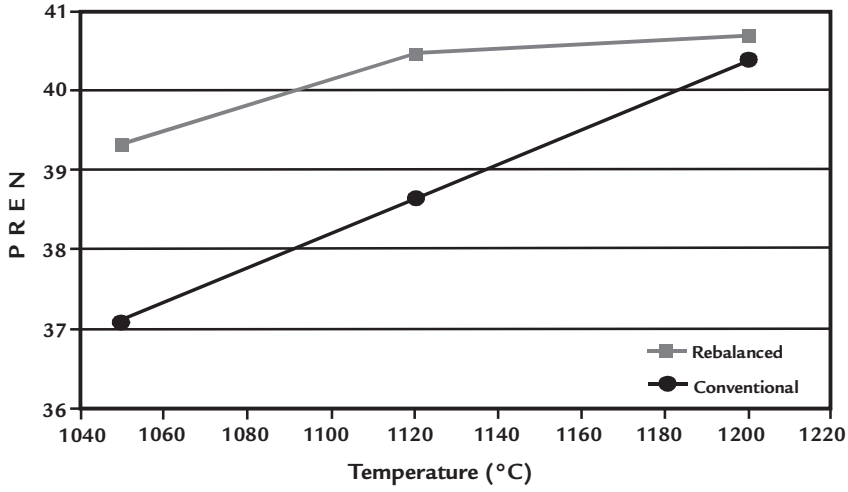

Figure 14
Total PREN number for the Conventional and Rebalanced steels calculated by Thermo-Calc.

Sample	Conventional (J)	Rebalanced (J)
Mid Radius (∅ 152.40 mm)	101.4	215.3 ± 35.7

Table 8
Longitudinal impact absorbed energy (Charpy V) of conventional and balanced steels at -46°C (minimum required is 45 J).

4. Conclusions

The present study on large diameter bars produced in super-duplex stainless steel UNS S 32760 has shown that the pitting corrosion resistance can be improved using alloy design tools like phase numerical simulation software Thermo-Calc as a base to rebalance the alloy. It was demonstrated that the presence of inter-granular Cr_2N in ferrite acts as a pitting initiation reducing the critical pitting temperature – CPT of the alloy even though the mechanical properties and toughness are still above the acceptance criteria. Besides the alloy composition balance, the processing parameters as finishing rolling/forging temperatures and solution annealing temperature are determinants to reach the desired mechanical and corrosion properties as required by the Norsok standard MDS D57 Revision 3 in large diameter rolled bars up to 152.40 mm.

5. References

AMERICAN SOCIETY FOR TESTING AND MATERIALS. G 48-03: Standard test methods for pitting and crevice corrosion resistance of stainless steels and related alloys by use of ferric chloride solution. ***Annual Book of ASTM Standards***. Philadephia: ASTM, 2009.

AMERICAN SOCIETY FOR TESTING AND MATERIALS. G 150-99: Standard test method for electrochemical critical pitting temperature testing of stainless steels. ***Annual Book of ASTM Standards***. Philadephia: ASTM, 2009.

BARBOSA, C. A. A contribuição das LRCs no revestimento de poços. ***Corrosão e Proteção***, p.11-13, Novembro/Dezembro, 2008.

DUPLEX 2007. ***CD-ROM Proceeding***. Italy: Associazione Italiana di Metalurgia, June, 2007.

ESTEBAN, M.P. et al. Anisotropy in the mechanical properties of two duplex stainless steels with different phase balance. ***European Stainless Steel Conference***, p.547-553, 2008.

INTERNATIONAL MOLYBDENUM ASSOCIATION (IMOA). ***Practical guidelines for fabrication of duplex stainless steel***. London: IMOA, 2009. 64p.

LØVLAND, P. Super stainless steels. ***Stainless Steel Europe***, p.28-37, november, 1993.

NILSSON, J. O., KANGAS, P. Influence of phase transformations on mechanical properties and corrosion properties in duplex stainless steels. ***Stainless Steel World***, p.56-59, may, 2007.

Paper submitted to INOX 2010- 10th Brazilian Stainless Steel Conference, September 20-22, Rio de Janeiro, Brazil. Revised accepted December, 05, 2012.